ELSEVIER

Journal of Power Sources 90 (2000) 196–200

JOURNAL OF POWER SOURCES

www.elsevier.com/locate/jpowsour

Cycle characterizations of $LiM_xMn_{2-x}O_4$ (M = Co, Ni) materials for lithium secondary battery at wide voltage region

Masaki Okada, Yun-Sung Lee, Masaki Yoshio *

Department of Applied Chemistry, Saga University, 1 Honjo, Saga 840-8502, Japan

Received 24 September 1999; received in revised form 16 January 2000; accepted 19 February 2000

Abstract

$LiM_xMn_{2-x}O_4$ (M = Co, Ni) materials have been synthesized by a melt-impregnation method using γ-MnOOH as the manganese source. Highly crystallized $LiM_xMn_{2-x}O_4$ compounds were synthesized at a calcination temperature of 800°C for 24 h in air. All compounds show a single phase except for $LiNi_{0.5}Mn_{1.5}O_4$ based on the X-ray diffraction (XRD) diagram. With the increase of the doping content from 0.1 to 0.5, the capacity of doping materials decreases mainly in the 4 V region.

Although $LiM_{0.5}Mn_{1.5}O_4$ (M = Co, Ni) compound shows a small capacity in the (3 + 4) V region compared with parent $LiMn_2O_4$, it is a very effective material in reducing capacity loss in the 3 V region that is caused by the Jahn–Teller distortion. The doping of Co and Ni ions in the $LiMn_2O_4$ cathode material promotes the stability of this structure and provides an excellent cyclability.

Keywords: Spinel; Metal ion-doped spinel; Cyclability; Jahn–Teller distortion; Lithium secondary battery

1. Introduction

The layered oxide materials, $LiMO_2$ (M = Co, Ni), have been investigated as cathode materials for lithium secondary batteries. $LiCoO_2$ is currently used as a cathode material of the commercial lithium ion battery. Also, $LiMn_2O_4$ has been widely investigated because of its cost performance, environmental merit and easy preparation method compared with other cathode materials [1,2].

Although the $LiMn_2O_4$ spinel shows an excellent cycle performance in the 4 V region at room temperature, stoichiometric $LiMn_2O_4$ cell indicates a significant capacity fading when it is used in the (3 + 4) V region. The two distinct plateaus at 4.05 and 4.15 V are usually displayed when the lithium insertion/extraction in $Li_xMn_2O_4$ is up to $x = 1.0$. The insertion of extra Li ($x > 1$) results in a sharp voltage drop to the 2.8 V plateau, which corresponds to the coexisting phase of the cubic $LiMn_2O_4$ and the tetragonal $Li_2Mn_2O_4$ ($x = 2$). This phenomenon is called the Jahn–Teller distortion and is caused by the presence of Jahn–Teller ions (Mn^{3+}) [3,4].

The Jahn–Teller transition, which is related to the large volume change in the unit cell, provides the origin of the large capacity fading measured in the $Li/Li_xMn_2O_4$ cells when cycled over the $0 < x < 2$ range[4–6]. It is also well known that full lithium insertion/extraction process has led to the gradual decay of its original structure and $LiMn_2O_4$ has indicated fast capacity loss when used at the (3 + 4) V region [7].

However, we have found that $LiMn_2O_4$ synthesized using γ-MnOOH as the manganese source was better stabilized upon cycling; nevertheless, it was cycled at (3 + 4) V region. We also succeeded in synthesizing the $LiM_xMn_{2-x}O_4$ materials with excellent cycle retention rate as well as a large capacity in the 4.2–2.0 V range. Therefore, we report the characterizations of $LiM_xMn_{2-x}O_4$ (M = Co, Ni) materials and the reason why they show large discharge capacity and good cyclability in the wide voltage region.

2. Experimental

The cathode materials were synthesized using LiOH, Co_3O_4, $Ni(OH)_2$ and γ-MnOOH as starting materials. These materials were mixed in appropriate ratios ($x =$

* Corresponding author. Tel.: +81-952-28-8673; fax: +81-952-28-8591.

E-mail address: yoshio@ccs.ce.saga-u.ac.jp (M. Yoshio).

0378-7753/00/$ - see front matter
PII: S0378-7753(00)00410-9

0.1–0.5) and ground in a mortar. These compounds were precalcined at 470°C for 5 h in air, followed by heating at 800°C for 24 h by the melt-impregnation method [8,9].

The powder X-ray diffraction (XRD, Rint 1000, Rigaku) using Cu K_α radiation was performed at room temperature to identify the crystalline phase of the powders that were prepared with different Co or Ni contents.

The electrochemical characterizations were performed using CR2032 coin-type cells. The method of assembling the cell was as follows: the cathode was 20 mg of accurately weighed active material and 13 mg of conductive binder. It was pressed on a 25-mm^2 stainless steel mesh used as the current collector at 300 kg/cm^2 and dried at 200°C for 5 h in an oven. This cell consisted of a cathode and a lithium metal anode (Cyprus Foote Mineral) separated by a porous polypropylene film as the separator (Celgard 3401). The electrolyte used was a 1-M $LiPF_6$-ethylene carbonate (EC)/dimethyl carbonate (DMC) (1:2 by volume). The cell was assembled in an argon-filled dry box and tested at room temperature. The charge and discharge current density was 0.4 mA/cm^2 with cut-off voltages of 2.0 to 4.2 V (vs. Li/Li^+).

3. Results and discussion

Fig. 1 shows the XRD patterns of the $LiCo_xMn_{2-x}O_4$ and $LiNi_xMn_{2-x}O_4$ samples when x is from 0.0 to 0.5. These samples were synthesized at 800°C for 24 h in air. $LiCo_xMn_{2-x}O_4$ samples show a single-phase spinel ($Fd\bar{3}m$) and no impurities over the whole range. $LiNi_xMn_{2-x}O_4$ shows the same pattern, as compared with $LiCo_xMn_{2-x}O_4$ until x is 0.3. However, it shows a slightly different behavior in the XRD pattern when x is 0.5. The other peaks that correspond with NiO is shown in Fig. 1(e). This means that the substituted Ni ion in the spinel structure cannot form a solid solution perfectly when x is 0.5. It may be very difficult to prepare the Ni doped spinel via the solid state reaction. Amine et al. [10] reported that $LiNi_xMn_{2-x}O_4$, which was synthesized by conventional solid-state method, is always observed in NiO peaks when the nickel amount is over 0.2. It is needed in several re-calcination processes at high temperature to obtain pure nickel-doped spinel. However, in our research, the NiO peaks appeared slightly when x was only 0.5, and the peak was very weak. We also confirmed that the NiO impurities could be removed completely by the re-calcination process. It means that the melt-impregnation method (a kind of solid-state method) is more effective than the conventional solid-state method to obtain homogeneous compounds [10].

The $\sin\theta/\lambda$–$\beta\cos\theta/\lambda$ plot of the $LiCo_xMn_{2-x}O_4$ compound is shown in Fig. 2. The following equation can be introduced using the Scherrer equation [11,12]

$$\beta\cos\theta/\lambda = 1/\varepsilon + 2\eta(\sin\theta/\lambda)$$

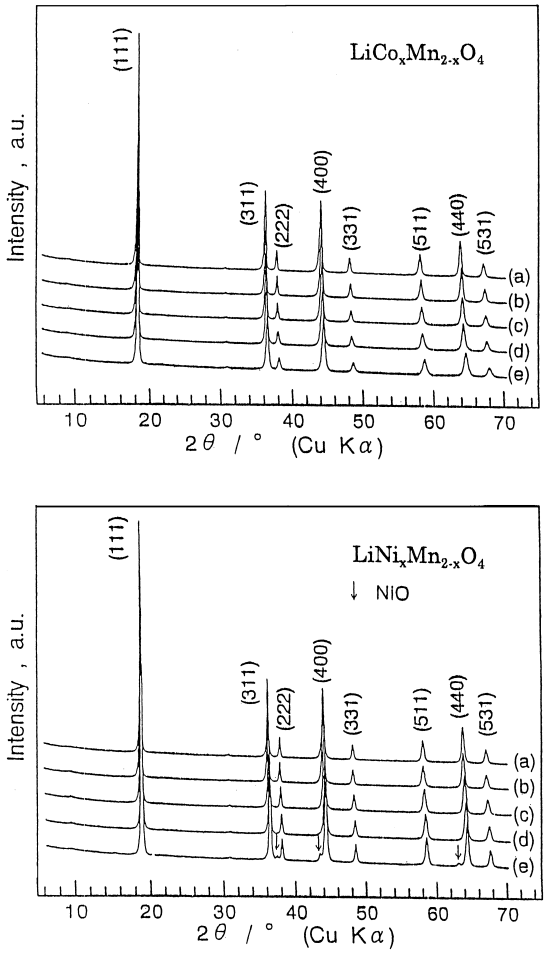

Fig. 1. XRD patterns of $LiCo_xMn_{2-x}O_4$ and $LiNi_xMn_{2-x}O_4$ compounds; (a) $x = 0.0$, (b) $x = 0.1$, (c) $x = 0.2$, (d) $x = 0.3$, (e) $x = 0.5$.

where β is the integral width of the intensity peak, η indicates the strain of the crystalline structure, and ε means the crystallite size. The λ value is 1.5405 Å (Cu K_α). It was clarified that the capacity loss on the cycling at (3 + 4) V region decreased with increase in the slope value of Hall plot ($= 2\eta$ value) from the results of this crystal analysis (see Figs. 2 and 5(a)). $LiMn_2O_4$, which was synthesized using γ-MnOOH as the Mn source, has a larger η value ($\eta = 1.46 \times 10^{-3}$) than other Mn sources. The η values of $LiMn_2O_4$ using CMD and EMD are 0.00×10^{-3} and 0.45×10^{-3}, respectively. It means that $LiMn_2O_4$ (using γ-MnOOH) has a smaller crystallite size and higher strain in the structure. All metal ion-doped spinels in this research show a higher η value than that of the other $LiMn_2O_4$ (using CMD and EMD) and increase η value in proportion to the doping content. Therefore, we considered that the crystallite size and the strain in the structure were important factors for the structure change of $LiMn_2O_4$ and $LiM_xMn_{2-x}O_4$ materials. These properties also can bring about different physical characterizations and electrochemical behaviors in the wide voltage region.

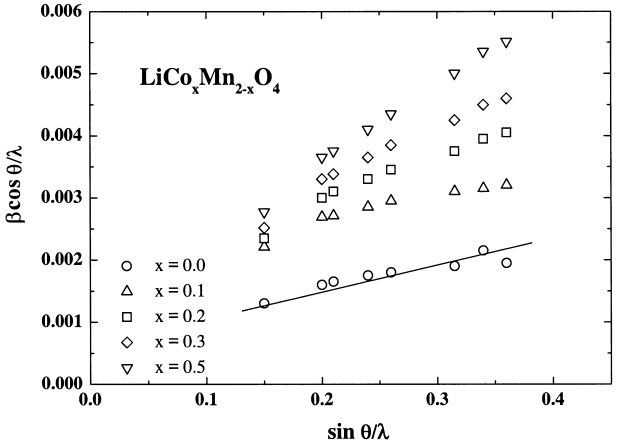

Fig. 2. The $\sin\theta/\lambda - \beta\cos\theta/\lambda$ plot of $LiCo_xMn_{2-x}O_4$ compounds. η value was 1.9×10^{-3} ($x = 0.1$), $3.321.9\times10^{-3}$ ($x = 0.2$), $4.131.9\times10^{-3}$ ($x = 0.3$) and $5.491.9\times10^{-3}$ ($x = 0.5$).

Fig. 3 shows the first charge–discharge curves of the Li/1M $LiPF_6$-EC/DMC/$LiCo_xMn_{2-x}O_4$ and $LiNi_x$-$Mn_{2-x}O_4$ cells when x is 0.1 and 0.5. It was galvanostatically carried out at a constant charge–discharge current density of 0.4 mA/cm^2 between 2.0 and 4.2 V. The $LiCo_{0.1}Mn_{1.9}O_4$ cell shows each distinct plateau at 3 and 4 V. According to the increase in the Co content, the total capacity of the $LiCo_xMn_{2-x}O_4$ compound decreases step by step and capacity loss almost occurs in the 4 V region. Unlike the Co-substituted compound, the $LiNi_{0.5}Mn_{1.5}O_4$ powder shows a different voltage profile. Although $LiNi_{0.1}Mn_{1.9}O_4$ exhibits each plateau in the (3 + 4) V region as Co-doped material, $LiNi_{0.5}Mn_{1.5}O_4$ cell shows only one plateau in the 3 V region. Because the spinel must be electrically compensated by the oxidation of Mn^{3+} to Mn^{4+}, the valence of manganese ion in this material changes to Mn^{4+}. Some groups also have been explained as follows [10,13]: because all Mn ions in $LiNi_{0.5}Mn_{1.5}O_4$ are tetravalent, an oxidization reaction that changes Mn^{4+} to Mn^{3+} by the electrochemical reaction at 4 V (vs. Li/Li^+) is very difficult to occur. Therefore, the $LiNi_{0.5}Mn_{1.5}O_4$ cell does not show a 4 V plateau in the (3 + 4) V region. It means that only Mn^{3+} ion contributes to the charge/discharge capacity in the 4 V region. The charge/discharge capacity in the 4 V region decreases with the increase in x value. We confirmed that our results agreed with that of the other group [10].

We suggest another possibility as to why it shows a different initial capacity between the Co- and Ni-doped material as shown in Fig. 3. When metal doped ions were substituted into the spinel structure, the oxidation states of Co and Ni are trivalent and divalent, respectively. It has already been revealed using X-ray photoelectron spectroscopy (XPS) by Amine et al. [10]. The substituted Ni ion induces a higher average manganese oxidation state than that of the Co-doped spinel. We have already reported

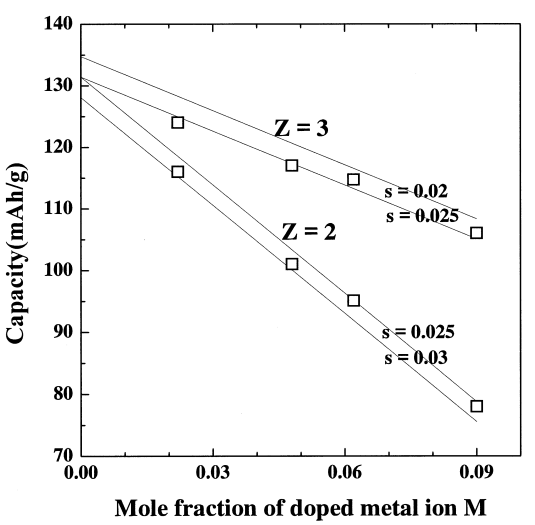

Fig. 3. Theoretical capacity for divalent ($z = 2$) and trivalent ($z = 3$) metal ion-doped spinel and measured capacity of Co and Ni-doped spinel; $[Li_x\square_{1-x}]_{8a}[Mn(III)_pMn(IV)_qM(z)_r\square_s]_{16d}O_4$, s = vacancy content.

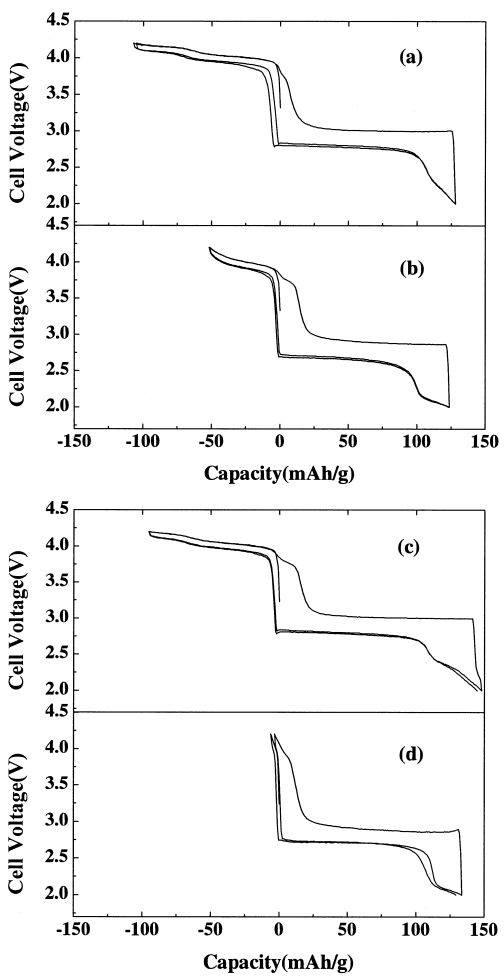

Fig. 4. The first charge–discharge curves for Li/1M $LiPF_6$-EC/DMC/$LiM_xMn_{2-x}O_4$ cells with various doping contents. (a) $LiCo_{0.1}Mn_{1.9}O_4$, (b) $LiCo_{0.5}Mn_{1.5}O_4$, (c) $LiNi_{0.1}Mn_{1.9}O_4$, (d) $LiNi_{0.5}Mn_{1.5}O_4$. Cycling was carried out at a constant charge–discharge current density of 0.4 mA/cm^2 between 2.0 and 4.2 V.

the calculation method for the theoretical capacity of the metal ion-doped spinels [14]. The theoretical capacity increases with increasing oxidation number of the doped metal ion at the same doping content. Fig. 4 shows the relations of the theoretical capacity and doped metal ion of the $LiM_xMn_{2-x}O_4$ compounds. The cycle test was performed in the 4 V region (3.5–4.5 V) and the current rate was 0.4 mA/cm^2. This result explains well the reason why $LiCo_xMn_{2-x}O_4$ has to indicate a much higher capacity than the Ni-doped compound. Because the valence states of Co and Ni are different, each compound showed such a different cycle characterization. We confirmed that our results are coincident with theoretical values, as shown in Fig. 4. Furthermore, we found that the $LiNi_xMn_{2-x}O_4$ compound has a higher the number of vacancy in this structure ($0.025 < s < 0.03$). The vacancy content in the 16d site for Co-doped materials is lower than that of Ni-doped materials. It can also be a reason that the $LiCo_xMn_{2-x}O_4$ material shows a larger discharge capacity than the $LiNi_xMn_{2-x}O_4$ compound.

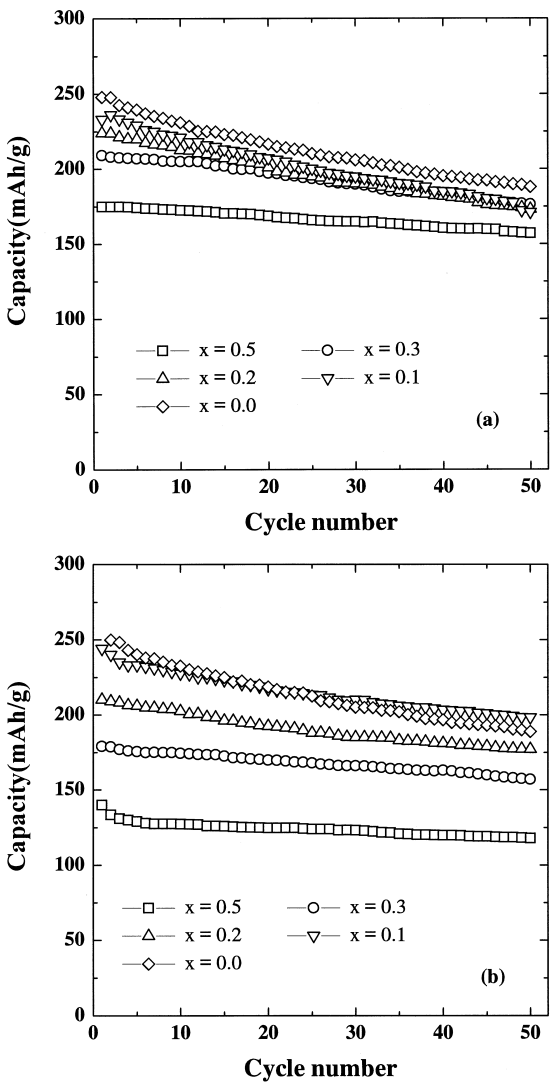

Fig. 5. The plot of specific discharge capacity vs. number of cycles for the Li/1M $LiPF_6$-EC/DMC/$LiM_xMn_{2-x}O_4$ cells with various doping contents. (a) $LiCo_xMn_{2-x}O_4$ (b) $LiNi_xMn_{2-x}O_4$. Cycling was carried out at a constant charge–discharge current density of 0.4 mA/cm^2 between 2.0 and 4.2 V.

Fig. 5(a) shows plots of the discharge capacity vs. the cycle number of a test cell using the $LiCo_xMn_{2-x}O_4$ compound. The stoichiometric $LiMn_2O_4$ delivered a discharge capacity of 248.5 mA h/g, while the last capacity after the 50th cycle was 188 mA h/g. However, $LiCo_{0.5}Mn_{1.5}O_4$ delivered 175 mA h/g and 157.2 mA h/g. The cycle retention rate increases from 75.8% ($x = 0.0$) to 90% ($x = 0.5$). Fig. 5(b) shows the cycle characterization of the $LiNi_xMn_{2-x}O_4$ cell at various doping contents. Although the $LiNi_{0.1}Mn_{1.9}O_4$ powder shows a different cycle behavior in all compounds, the cycle performance of each compound enhances accordingly as the nickel content increases. $LiM_xMn_{2-x}O_4$ (M = Co, Ni) materials showed an excellent cycle retention rate as well as high discharge capacity. The stability in charge–discharge cycling increased with increase in η value. We concluded that the crystallite size and the strain in the structure were important factors for the structure change of $LiMn_2O_4$ from cubic to tetragonal phase in the charge–discharge process.

Some researchers announced that $LiMn_2O_4$-based materials shows poor cyclability in the 3 V region, which transforms the cubic symmetry of the spinel phase to a tetragonal symmetry by the Jahn–Teller distortion [15]. We reported here that $LiM_xMn_{2-x}O_4$ materials, which were synthesized using γ-MnOOH, show excellent cyclability as well as large discharge capacity; nevertheless, it was tested in the (3 + 4)V region. Therefore, we suggest that $LiM_xMn_{2-x}O_4$ (M = Co, Ni), which was synthesized using γ-MnOOH, can be a very effective cathode material to reduce the Jahn–Teller distortion in the 3 V region.

4. Conclusions

$LiM_xMn_{2-x}O_4$ (M = Co, Ni) materials were synthesized by a melt-impregnation method. They were calcined at 800°C for 24 h in air atmosphere. All compounds show a pure single phase except for the $LiNi_{0.5}Mn_{1.5}O_4$ compound, which shows NiO peaks in the XRD patterns. These materials have a smaller crystallite size and higher strain than that of the pure $LiMn_2O_4$. The cycle retention rate of the $LiCo_{0.5}Mn_{1.5}O_4$ increased from 75.8% ($x = 0.0$) to 90% ($x = 0.5$).

Co and Ni doping materials show a different cycle behavior in the (3 + 4) wide voltage region because they have different average oxidation states. Doping of Co and Ni ions into the $LiMn_2O_4$ compound is a very effective method for improving its structural stability and increasing the capacity retention rate during cycling.

References

[1] K. Mizushima, P.C. Jones, P.J. Wiseman, J.B. Goodenouh, Mater. Res. Bull. 15 (1980) 783.
[2] C. Plichata, M. Salomon, S. Slane, M. Uchiyoma, B. Chua, W.B. Ebner, H.W. Lin, J. Power Sources 21 (1987) 25.
[3] D. Guyomard, J.M. Tarascon, Solid State Ionics 69 (1994) 222.
[4] Y. Xia, H. Takeshige, H. Noguchi, M. Yoshio, J. Power Sources 56 (1995) 61.
[5] T. Ohzuku, J. Kato, K. Sawai, T. Hirai, J. Electrochem. Soc. 138 (1991) 2556.
[6] R.J. Gummow, A. de Kock, M.M. Thackeray, Solid State Ionics 69 (1994) 59.
[7] J.M. Tarascon, E. Wang, F.K. Sehokoohi, J. Electrochem. Soc. 138 (1991) 2859.
[8] Y. Xia, H. Takeshige, H. Noguchi, M. Yoshio, J. Power Sources 56 (1995) 61.
[9] Y. Xia, M. Yoshio, J. Power Sources 57 (1995) 125.
[10] K. Amine, H. Tukamoto, H. Yasuda, Y. Fujita, J. Electrochem. Soc. 143 (1996) 1607.
[11] W.H. Hall, J. Inst. Met. 75 (1950) 1127.
[12] L. Hernan, J. Morales, L. Sanchez, J. Santos, Solid State Ionics 118 (1999) 179.
[13] Li. Guohua, H. Ikuta, T. Uchida, M. Wakahara, J. Electrochem. Soc. 143 (1996) 178.
[14] Y.M. Todorov, Y. Hideshima, H. Noguchi, M. Yoshio, J. Power Sources 77 (1999) 198.
[15] M.M. Thackeray, A. de Kock, M..H. Roussow, D.C. Liles, R. Bittihn, D. Hoge, J. Electrochem. Soc. 139 (1992) 363.